JOURNAL OF GUIDANCE, CONTROL, AND DYNAMICS
Vol. 30, No. 4, July–August 2007

Linear Parameter-Varying Antiwindup Compensation for Active Microgravity Vibration Isolation

Feng Zhang,* Karolos M. Grigoriadis,† and Ian J. Fialho‡
University of Houston, Houston, Texas 77204

DOI: 10.2514/1.27958

In this paper a linear parameter-varying antiwindup approach is examined to provide antiwindup compensation for adaptive active microgravity vibration isolation. For such systems, antiwindup protection is essential because of actuator saturation in response to inertially based forces acting on the isolated platform. For the example presented in this paper, a static antiwindup compensator scheduled based on the measurement of the rack displacement is designed so that it applies a correcting signal only when the control force is saturated. The linear parameter-varying antiwindup scheme is combined with a linear parameter-varying controller that shifts its focus from a soft setting to a stiff setting depending on the need for acceleration minimization or relative displacement reduction to prevent the isolation rack from bumping onto its hard stops. The performance of the overall closed-loop system is validated by extensive simulations that demonstrate the need and benefits of the linear parameter-varying antiwindup compensation.

I. Introduction

ACTIVE vibration isolation has become an important enabling technology in a wide range of engineering applications ranging from space science to the machining of precision parts. Recent applications, such as the microgravity isolation in space and the lithography of microelectronic devices, impose extremely stringent vibration isolation requirements resulting in the need for novel optimization-based active vibration control schemes. Microgravity vibration isolation is a critical function onboard the International Space Station (ISS). A main objective of ISS is to serve as a premier on-orbit laboratory for conducting acceleration-sensitive scientific research in diverse disciplines, such as material science, combustion, fundamental physics, chemical processing, fluid mechanics, and biotechnology. However, due to a variety of external and internal vibrations and acoustic excitations the ISS acceleration environment is expected to significantly exceed the micro-g specifications of many acceleration-sensitive experiments. The strict microgravity isolation requirements along with the wide range of the excitation frequencies make this an extremely challenging vibration isolation problem. Low-frequency excitations (less than 0.001 Hz) are due to gravity gradient forces and atmospheric drag. Intermediate-range vibrations (from 0.001 to 1 Hz) are mostly transient in nature due to astronaut motion and thruster firings. High-frequency vibrations (above 1 Hz) are caused by sinusoid steady-state sources, such as pumps, compressors, exercise equipment and fans, as well as transient sources, such as impacts. Both classical and modern control approaches have been proposed recently to address the microgravity vibration isolation control problem [1–5].

In [5], a linear parameter-varying (LPV) controller was designed to provide adaptive microgravity vibration isolation performance. The designed adaptive LPV controller provides improved isolation and position control over the full range of operating conditions via the use of parameter-dependent weighting functions. However, because the controller is of high gain and high bandwidth, disturbances such as inertially based forces applied to the isolated platform cause the controller to command values to the actuator that exceed its saturation limits. During such events, isolation performance is degraded and modifications of the nominal control algorithm are necessary to keep the system well behaved.

Actuator saturation exists in almost all engineering control systems. Because of saturation, the actual plant input is different from the controller output. This discrepancy is called controller windup [6]. Because actuator saturation is ignored in linear control design, controller windup could result in degradation from expected linear performance, large overshoot, or possible instability [7]. As a result, actuator saturation has received increasing attention from the systems and controls research community [8–10]. However, due to the complexity of the antiwindup problem, early antiwindup schemes were mostly heuristic in nature. Only in the last decade has the problem been addressed in a more systematic way with stability guarantees and clear performance specifications.

A popular approach to saturating control is the antiwindup method that employs a two-step design procedure. The idea here is to first design the linear controller by ignoring the saturation nonlinearity and then add antiwindup compensation to minimize the adverse effects of saturation on closed-loop performance. In [11], a rigorous definition of antiwindup compensation was provided in terms of $\mathcal{L}_2$ stability and performance. The performance of the antiwindup augmentation is characterized by the $\mathcal{L}_2$ norm of the deviation between the actual response of the augmented closed-loop system and the ideal response of the unconstrained system. In [12], linear matrix inequality (LMI)-based antiwindup compensator synthesis with input–output quadratic stability and performance guarantees for a stable system is presented. Most previous antiwindup compensator designs are only applicable to open-loop stable linear time-invariant (LTI) systems, hence limiting their usefulness in practical problems. When the system is nonlinear and open-loop unstable, the control synthesis problem becomes very difficult to solve and therefore global stabilization cannot be achieved [9,13]. To solve the antiwindup problem for such systems, the results in [12] are extended to unstable systems in [14] by restricting the bound on input nonlinearity to a small conic sector, thereby leading to regional stability. Moreover, the antiwindup control scheme for LTI plants in [15] is generalized to linear parameter-varying systems in [16] because of the relevance of LPV control to nonlinear systems. An alternative systematic antiwindup approach that can be brought to bear on the nonlinear and open-loop unstable system is to embed it within a larger LPV problem; see [10,14] for details. This allows

Received 21 September 2006; revision received 3 March 2007; accepted for publication 12 April 2007. Copyright © 2007 by the American Institute of Aeronautics and Astronautics, Inc. All rights reserved. Copies of this paper may be made for personal or internal use, on condition that the copier pay the $10.00 per-copy fee to the Copyright Clearance Center, Inc., 222 Rosewood Drive, Danvers, MA 01923; include the code 0731-5090/07 $10.00 in correspondence with the CCC.

*Graduate Student, Department of Mechanical Engineering; fzhang2@gmail.com.

†Professor, Department of Mechanical Engineering; karolos@uh.edu. Associate Fellow AIAA (Corresponding Author).

‡Adjunct Professor, Department of Mechanical Engineering; ian.j.fialho@boeing.com.

standard LPV stability and performance methods to be applied to the problem. However this single-step approach may result in conservative designs.

In this paper, the LPV antiwindup technique developed in [16] is applied for antiwindup protection of a microgravity vibration isolation system controlled by an adaptive LPV controller as proposed in [5]. There are some main differences of the application considered in the present paper compared with the aircraft control example examined in [16]. For the antiwindup problem considered here, the plant is marginally stable LTI, whereas the controller is LPV. A static, that is, no dynamic state, LPV antiwindup compensator is designed to augment the nominal LPV controller. A static antiwindup compensator is more practical than full or reduced-order dynamic ones because it is easier to implement. Also a static antiwindup compensator stops influencing the nominal system as soon as the controller comes out of saturation. Parameter-dependent Lyapunov functions are used for the antiwindup compensator design to guarantee the best possible performance. Numerical simulations are used to demonstrate the effectiveness of the combined LPV antiwindup compensation scheme in an adaptive active microgravity isolation problem.

The organization of the paper is as follows: Section II introduces the LPV antiwindup compensator design method. Antiwindup compensator synthesis for the adaptive active microgravity isolation problem is presented in Sec. III. Section IV discusses the LPV antiwindup design results and simulation studies for a specific microgravity isolation problem. Finally concluding remarks are found in Sec. V.

II. Antiwindup Synthesis for Linear Parameter-Varying Systems with Input Saturation

The antiwindup synthesis approach used in this paper is based on robust stability and performance results for sector-bounded uncertainties and it has been systematically presented in [16]. The antiwindup control structure is shown in Fig. 1, where $P(\theta)$ is the linear parameter-varying plant described by

$$\begin{bmatrix} \dot{x}_p \\ e \\ y \end{bmatrix} = \begin{bmatrix} A_p(\theta) & B_{p1}(\theta) & B_{p2}(\theta) \\ C_{p1}(\theta) & D_{p11}(\theta) & D_{p12}(\theta) \\ C_{p2}(\theta) & D_{p21}(\theta) & D_{p22}(\theta) \end{bmatrix} \begin{bmatrix} x_p \\ d \\ \sigma(u) \end{bmatrix} \tag{1}$$

where $x_p \in R^{n_p}$ is the plant state, $y \in R^{n_y}$ is the measurement, $\sigma(u) \in R^{n_u}$ is the saturated control input, $e \in R^{n_e}$ is the controlled output, and $d \in R^{n_d}$ is disturbance input. The parameter vector θ is not known a priori but can be measured in real time. It is assumed that θ takes values in a compact set and has a bounded variation rate. The actuator nonlinearity $\sigma(u)$ under consideration is defined as follows:

$$\sigma(u_i) = \begin{cases} u_i & |u_i| < u_i^{\max} \\ \operatorname{sgn}(u_i) u_i^{\max} & |u_i| \geq u_i^{\max} \end{cases}, \qquad i = 1, \ldots, n_u$$

where sgn(.) denotes the signum function. Following standard two-step antiwindup procedures, a nominal practical (rate independent) LPV controller $K_{\text{nom}}(\theta)$ is designed first, ignoring the input nonlinearity. The nominal LPV controller $K_{\text{nom}}(\theta)$ is designed to stabilize the open-loop system when no input saturation exists, and its design determines the nominal performance of the closed-loop system. The structure of this nominal controller is

$$\begin{bmatrix} \dot{x}_k \\ u \end{bmatrix} = \begin{bmatrix} A_k(\theta) & B_k(\theta) \\ C_k(\theta) & D_k(\theta) \end{bmatrix} \begin{bmatrix} x_k \\ y \end{bmatrix} + \begin{bmatrix} v_1 \\ v_2 \end{bmatrix} \tag{2}$$

where $x_k \in R^{n_k}$ is the controller state. The inputs v_1 and v_2 are additional inputs added after the nominal design and are used for antiwindup augmentation. The LPV antiwindup compensator is of the form

$$\begin{bmatrix} \dot{x}_{\text{aw}} \\ v_1 \\ v_2 \end{bmatrix} = \begin{bmatrix} A_{\text{aw}}(\theta, \dot{\theta}) & B_{\text{aw}}(\theta) \\ C_{\text{aw}}(\theta, \dot{\theta}) & D_{\text{aw}}(\theta) \end{bmatrix} \begin{bmatrix} x_{\text{aw}} \\ q \end{bmatrix} \tag{3}$$

where $x_{\text{aw}} \in R^{n_{\text{aw}}}$ is the antiwindup compensation state. The adverse effect of input saturation is minimized in an $\mathcal{H}_\infty$ norm sense by using the LPV antiwindup compensator. By reducing the dead band nonlinearity $\Delta_i = 1 - [\sigma(u_i)/u_i]$ to $\operatorname{sect}[0, k_i]$ with $0 < k_i < 1$, regional stability for open-loop unstable systems can be obtained. The notation $\operatorname{sect}[0, k_i]$ denotes a conic sector $[0, k_i]$. The following result provides synthesis conditions for the antiwindup compensator [16].

Theorem 1: Consider scalars $0 < k_i < 1$, $i = 1, 2, \ldots, n_u$, and the LPV open-loop system $P(\theta)$ with a stabilizing nominal LPV controller $K_{\text{nom}}(\theta)$. If there exist a pair of positive-definite matrix functions $R_{11}(\theta)$, $S(\theta)$, and a diagonal matrix function

$$V(\theta) = \operatorname{diag}\{v_1(\theta), v_2(\theta), \ldots, v_{n_u}(\theta)\} > 0$$

satisfying

$$\begin{bmatrix} \begin{Bmatrix} R_{11}A_p^T + A_pR_{11} - \dot{R}_{11} \\ -2B_{p2}\Lambda^{-1}V(I - \Lambda^{-1})B_{p2}^T \end{Bmatrix} & * & * \\ \begin{Bmatrix} C_{p1}R_{11} \\ -2D_{p12}^{-1}\Lambda V(I - \Lambda^{-1})B_{p2}^T \end{Bmatrix} & \begin{Bmatrix} -\gamma I_{ne} \\ -2D_{p12}\Lambda^{-1}V(I - \Lambda^{-1})D_{p12}^T \end{Bmatrix} & * \\ B_{p1}^T & D_{p11}^T & -\gamma I_{n_d} \end{bmatrix} < 0 \tag{4}$$

$$\begin{bmatrix} SA + A^TS + \dot{S} & * & * \\ B_1^TS & -\gamma I_{n_d} & * \\ C_1 & D_{11} & -\gamma I_{n_e} \end{bmatrix} < 0 \tag{5}$$

$$\begin{bmatrix} R_{11}(\theta) & * \\ \begin{bmatrix} I_{n_p} \\ 0 \end{bmatrix} & S(\theta) \end{bmatrix} \geq 0 \tag{6}$$

where $\Lambda = \operatorname{diag}\{k_1, k_2, \ldots, k_{n_u}\}$, then there exists an n_pth-order antiwindup compensator $K_{\text{aw}}(\theta)$ to stabilize the closed-loop system and guarantee $\mathcal{L}_2$ gain performance $\|e\|_2 < \gamma\|d\|_2$ when the condition $|u_i| \leq [1/(1 - k_i)]u_i^{\max}$, $i = 1, 2, \ldots, n_u$ holds.

It can be seen that the antiwindup compensator (3) is essentially a rate dependent compensator that is not a practical compensator from an implementation viewpoint, when parameter-dependent Lyapunov

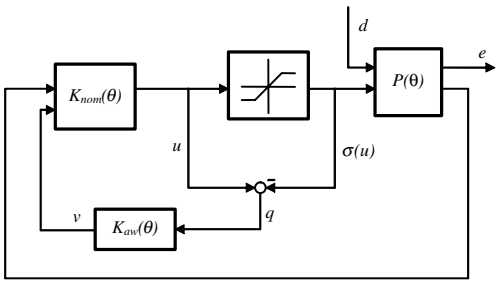

Fig. 1 Antiwindup controller structure.

functions are applied. However the rate dependence only enters the compensator matrices $A_{\rm aw}$ and $C_{\rm aw}$ so that the corresponding static compensator is a rate independent compensator. Such a compensator is preferable because it is easier to implement. The synthesis LMIs for the static antiwindup compensator can be obtained by enforcing $R = S^{-1}$. The following result provides the synthesis conditions for the static antiwindup compensator design.

Proposition 2: Consider scalars $0 < k_i < 1$, $i = 1, 2, \ldots, n_u$, and the LPV open-loop system $P(\theta)$ with a stabilizing nominal controller $K_{\rm nom}(\theta)$. If there exist a positive-definite matrix function $R(\theta)$ and a diagonal matrix function $V(\theta) = \text{diag}\{v_1, v_2, \ldots, v_{n_u}\} > 0$ satisfying

$$\begin{bmatrix} \begin{Bmatrix} R_{11}A_p^T + A_pR_{11} - \dot{R}_{11} \\ -2B_{p2}\Lambda^{-1}V(I-\Lambda^{-1})B_{p2}^T \end{Bmatrix} & * & * \\ \begin{Bmatrix} C_{p1}R_{11} \\ -2D_{p12}\Lambda^{-1}V(I-\Lambda^{-1})B_{p2}^T \end{Bmatrix} & \begin{Bmatrix} -\gamma I_{ne} \\ -2D_{p12}\Lambda^{-1}V(I-\Lambda^{-1})D_{p12}^T \end{Bmatrix} & * \\ B_{p1}^T & D_{p11}^T & -\gamma I_{n_d} \end{bmatrix} < 0 \tag{7}$$

$$\begin{bmatrix} AR + RA^T - \dot{R} & * & * \\ B_1^T & -\gamma I & * \\ C_1R & D_{11} & -\gamma I \end{bmatrix} < 0 \tag{8}$$

where

$$R = \begin{bmatrix} R_{11} & * \\ R_{12}^T & R_{22} \end{bmatrix}$$

then there exists a static antiwindup compensator $K_{\rm aw}(\theta)$ to stabilize the closed-loop system and guarantee $\mathcal{L}_2$ gain performance $\|e\|_2 < \gamma\|d\|_2$ when the condition $|u_i| \leqslant [1/(1-k_i)]u_i^{\max}$, $i = 1, 2, \ldots, n_u$ holds.

The above LMI conditions are infinite dimensional due to their dependence on the parameter vector θ. However they can be solved by standard gridding techniques; see [17] for example. After solving for the unknown R_{11}, S, and V, the antiwindup compensator gain

$$\Theta = \begin{bmatrix} A_{\rm aw} & B_{\rm aw} \\ C_{\rm aw} & D_{\rm aw} \end{bmatrix}$$

can be computed explicitly using Theorem 2 in [16].

Note that the synthesis condition for the antiwindup compensator is obtained by reducing the dead band nonlinearity $\Delta_i = 1 - [\sigma(u_i)/u_i]$ to sect $[0, k_i]$ with $0 < k_i < 1$ and then obtaining regional stability for open-loop unstable systems. This will restrict the magnitude of the control input signal u_i to be less than $[1/(1-k_i)]u_i^{\max}$. It is usually hard to verify condition $|u_i| \leqslant [1/(1-k_i)]u_i^{\max}$ because the $u_i's$ are the controller outputs. Using the results in [18], when there is no direct feedthrough from the disturbance to the system output, a domain of attraction and maximum size of disturbance can be estimated. However the estimated stability region could be conservative.

In the following section, the static antiwindup control synthesis is applied to provide antiwindup compensation in an adaptive active microgravity vibration isolation problem.

III. Antiwindup Compensator Design for Active Microgravity Isolation Control

In [5], an adaptive LPV controller with parameter-dependent performance requirements is designed for an active microgravity isolation system. A brief overview of the system description is provided here and the reader is referred to [5] for details. A schematic of the isolation system is shown in Fig. 2. The goal of the control design is to achieve a desired level of isolation between the base acceleration $\ddot{x}_{\rm off}$ and the inertial acceleration $\ddot{x}_{\rm on}$ of the isolated platform. Figure 3 shows a typical target isolation curve used for microgravity isolation devices on board the ISS. This figure defines the attenuation from the off broad translational acceleration magnitude to the on broad translational acceleration magnitude [3,4]. As can be seen the target isolation curve has a -20 dB/decade rolloff between 0.01 and 10 Hz, and remains constant at -60 dB above 10 Hz. Low frequency (less than 0.01 Hz) station disturbances cause relative motion between the rack and the station, and to prevent the rack from bumping into its hard stops, the control system must cause the rack to follow the motion of the station. Hence it is not desirable to attenuate low frequency disturbances, and this is captured by the hump in the curve below 0.01 Hz [4]. In addition, the isolated

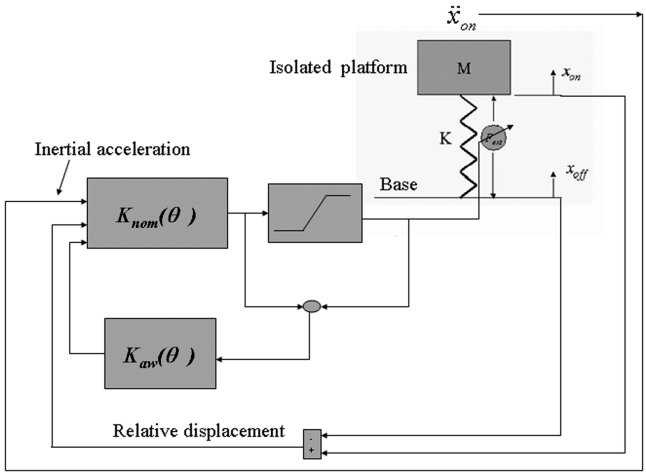

Fig. 2 Schematic of the isolation system.

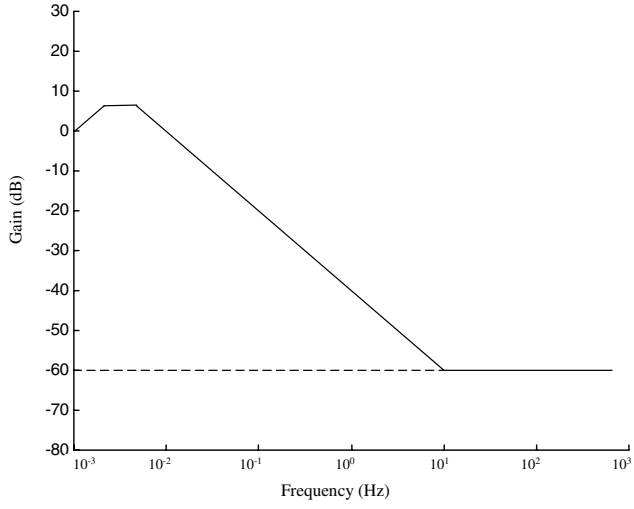

Fig. 3 Typical target microgravity isolation curve.

platform must operate in a limited rattle space of 0.5 in., and hence an additional design constraint is that the relative displacement $x_{\text{on}} - x_{\text{off}}$ does not exceed the 0.5 in. rattle-space limit to prevent the platform from bumping into its hard stops. To achieve these objectives the LPV controller is scheduled on the relative displacement θ_d. By scheduling on relative displacement, the LPV controller is able to shift its focus from a "soft" setting to a "stiff" setting depending on the need for acceleration minimization or relative displacement reduction to prevent bumping. Parameter-dependent weighting functions are used to achieve this objective. Weights that depend parametrically on the scheduling variables θ_d are appended to the basic LTI plant to create the generalized LPV plant for control design. For small displacements, the acceleration weight is large and the displacement weight is small, whereas for large displacements the displacement weight is large and the acceleration weight is small. Using this gradual weight change the controller shifts focus from acceleration minimization to displacement restriction depending on the position of the rack.

The parametric uncertainty in the spring constant K is taken into account in the LPV design by modeling it as an input divisive uncertainty [19]. This approach allows the controller to achieve excellent isolation performance over the full range of base motion environments, while at the same time preventing the isolated platform from exceeding its hard rattle-space limits. However because the controller is linear and aggressive, there are disturbances, such as inertially based forces acting on the isolated platform, that cause actuator saturation leading to significant degradation in isolation performance. Hence adding an antiwindup protection loop is necessary to ensure good isolation performance. The antiwindup method presented in Sec. II is used for the antiwindup compensator design.

In this paper, both the LPV controller and the LPV antiwindup compensator designs are carried out for a simplified model of a microgravity isolation system. In most of these isolation devices, kinematic and dynamic decoupling is employed to account for mass and inertia properties, stiffness cross coupling, and skewed location of actuators and sensors. This decoupling reduces the control design problem to six independent degrees of freedom (three translation and three rotation). Because of this, the single degree-of-freedom model is well justified from an engineering perspective, and is not merely a theoretical simplification [3,4]. However it should be emphasized that the proposed LPV control and antiwindup compensator design can be applied to multi-degree-of-freedom systems. The corresponding differential equation of motion is given by

$$M\ddot{x}_{\text{on}} + K(x_{\text{on}} - x_{\text{off}}) = F_{\text{ext}} \tag{9}$$

Defining $x_1 := x_{\text{on}} - x_{\text{off}}$, $x_2 := \dot{x}_{\text{on}} - \dot{x}_{\text{off}}$, $d := \ddot{x}_{\text{off}}$, $u = F_{\text{ext}}$, and $y := [\ddot{x}_{\text{on}}, x_1]^T$, Eq. (9) can be written in state-space form as follows:

$$\dot{x}_1 = x_2, \qquad \dot{x}_2 = -\frac{K}{M}x_1 + \frac{1}{M}u - d, \qquad y_1 = -\frac{K}{M}x_1 + \frac{1}{M}u$$

$$y_2 = x_1$$

The mass of the payload is assumed to be $M = 15$ slug and the spring constant K is assumed to lie between 0 and 20 lb/ft. The nominal controller design follows the same lines as in [5] and will not be repeated here.

Based on the above discussion, the system "seen" by the antiwindup controller is an LTI plant with the control loops closed by an LPV controller. The LPV controller designed in [5] is implemented using the linear interpolation of 11 grid-point controllers. According to Proposition 2, to design a static LPV antiwindup compensator, a set of matrix functions $R(\theta_d)$, $V(\theta_d)$, which solve the associated LMIs (7) and (8), and minimize the performance level γ, need to be found. These inequalities can be reduced to a set of finite dimensional LMIs, first by choosing appropriate basis functions that define the functional dependence of the matrix functions $R(\theta_d)$ and $V(\theta_d)$ on θ_d, and then by gridding the parameter space and solving the inequalities at the grid points [17]. However for validation purposes the constraints should be checked later with a much denser grid. Because of the special structure of this problem, that is, the plant is constant and the LPV controller is a linear combination of 11 grid controllers, we select the same form for the antiwindup design matrix functions as we did in the controller design as follows:

$$R(\theta_d) = R_0 + \theta_d R_1 + \frac{\theta_d^2}{2}R_2 \qquad V(\theta_d) = V_0$$

The rate bound of θ_d is chosen to be the same as the LPV controller design, that is, $[-0.025 \quad 0.025]$ ft/s. As $\dot{\theta}_d$ appear linearly in the LMIs (7) and (8), we only need to check the corresponding LMIs at the extreme points. To maximize the guaranteed stabilization region, the K value of sector-bounded input nonlinearity sect$[0, \Lambda]$ is chosen as close to 1 as possible with reasonable closed-loop performance level. For the antiwindup design at hand Λ was chosen as 0.9999. The LMIs are solved over the same parameter grid as was used in the original LPV controller design, and the solutions $R(\theta_d)$ and $V(\theta_d)$ are then verified to satisfy the constraints over a 101 point dense grid. The corresponding closed-loop $\mathcal{L}_2$-gain performance level is 9.58.

IV. Linear Parameter-Varying Antiwindup Design Results

The combined LPV control and antiwindup compensator designed as discussed above was verified through time-domain simulations. A nonlinear hysteresis model of the spring was used to validate the performance of the LPV controller and antiwindup compensator. The spring constant varies between 0 and 20 lbf/ft. The saturation limit for the actuator force is set to be $[-3 \quad 3]$ lb. Recall that the goal of the adaptive LPV controller designed in [5] is to minimize the acceleration of the isolated platform, subject to limited available rattle space. The goal of the antiwindup compensator design is to minimize isolation performance degradation in the presence of actuator saturation.

A representative inertial force profile (see Fig. 4) was applied to the isolated payload when the payload is located at the center of its rattle space to test the isolation performance when the displacement is small. In this regime the LPV controller is focusing on minimizing acceleration. The following three cases were simulated to demonstrate the effectiveness of the designed antiwindup compensator. The dash–dotted lines (case 1) in Figs. 5–7 show the acceleration, actuator force, and relative displacement responses of the nominal closed-loop system in the absence of saturation, that is, for the theoretical case where the actuator can provide unlimited control force. They serve as the benchmark nominal performance for comparison purposes. The dashed lines (case 2) in the figures show the same variables with the actuator force limited but with no antiwindup compensation. The solid lines (case 3) in the figures are the responses of the closed-loop system with the designed LPV antiwindup protection under actuator saturation. It can be seen that

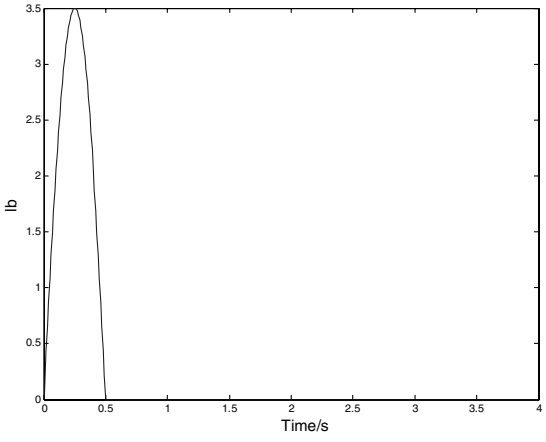

Fig. 4 Inertial force profile.

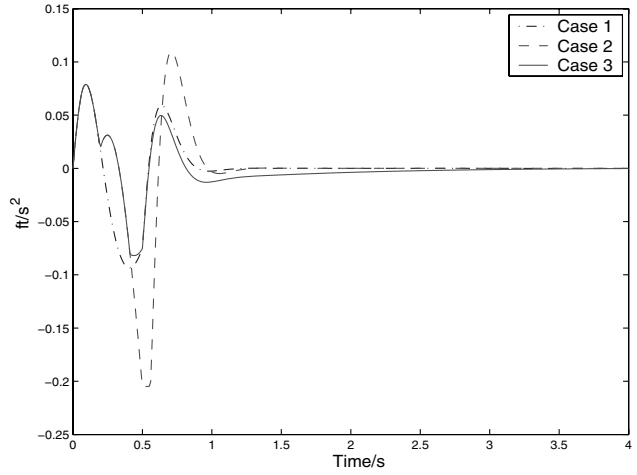

Fig. 5 Acceleration performance: unconstrained control, case 1; constrained control, case 2; constrained control with antiwindup, case 3.

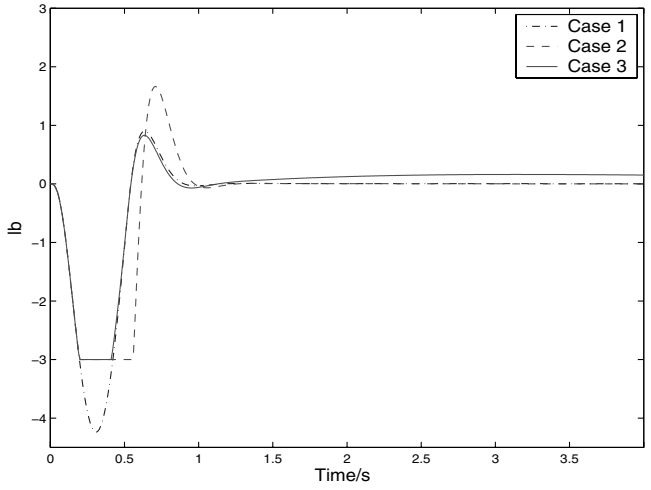

Fig. 6 Control force.

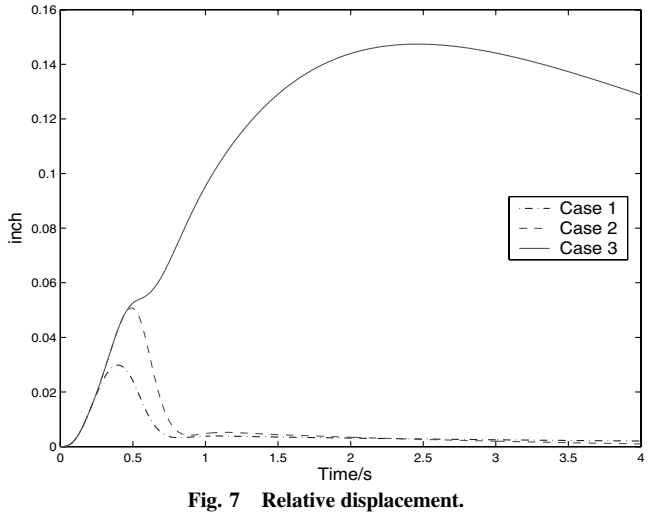

Fig. 7 Relative displacement.

the acceleration for case 2 is much larger than the acceleration for case 1, whereas for both cases, the relative displacements are under the displacement limit. Clearly, actuator saturation has degraded the isolation performance significantly so that it is necessary to add antiwindup protection to the system. The acceleration for case 3 is much smaller than the acceleration for case 2, which indicates that the isolation performance has been improved significantly by introducing the designed antiwindup compensator. It is evident that the acceleration responses are close for cases 1 and 3, which implies that the antiwindup compensator has successfully minimized performance degradation in the presence of saturation. Figure 6 indicates that the antiwindup compensator helps the controller get out of saturation early, and also prevents large overshoot. Figure 7 shows that the relative displacement for case 3 is larger than in case 2. This is expected because the payload is centered in its rattle space, and hence the controller is focusing on minimizing acceleration. However, it is still significantly below the displacement limit. Hence, it can be concluded that the antiwindup compensator improves the performance of the nominal controller under actuator saturation when the relative displacement is small.

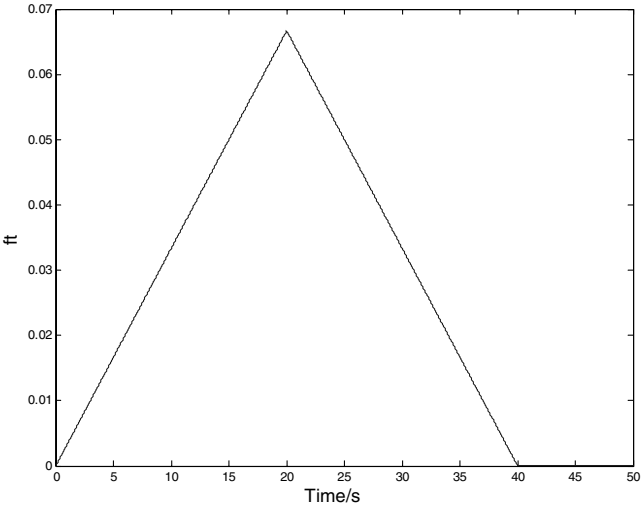

Fig. 8 Base motion disturbance profile.

To test the antiwindup performance when the relative displacement is large, an appropriate representative base motion displacement profile shown in Fig. 8 was applied to cause a large relative displacement. The same inertial force profile as before was then applied at 30 s and the same three cases were simulated for the above base motion displacement profile. Once again it is seen that the acceleration for case 3 is much smaller than case 2, while the difference of the displacements is very small; see Figs. 9–11. Clearly, the isolation performance is significantly improved by using the antiwindup compensator.

It is noted that application of the single-step LPV antiwindup scheme of [14] to this problem results in a conservative design where the target isolation curve (Fig. 3) and the antiwindup and performance objectives cannot be achieved simultaneously.

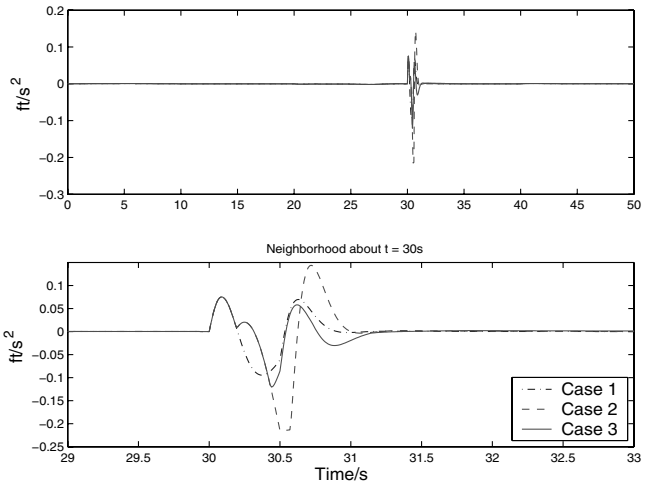

Fig. 9 Acceleration performance. The lower figure is a detailed view of the upper figure.

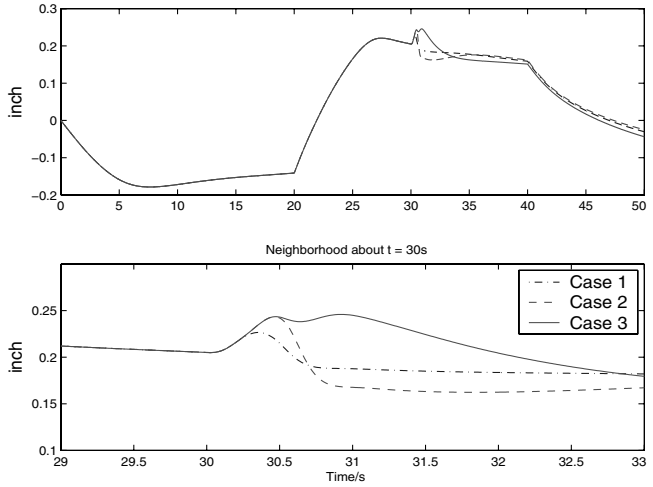

Fig. 10 Relative displacement.

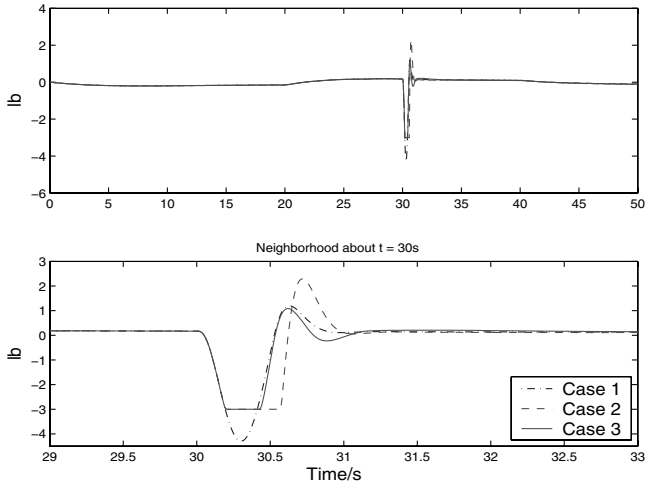

Fig. 11 Control force.

V. Conclusions

In this paper, an LPV antiwindup scheme proposed in [16] has been successfully applied to provide antiwindup protection for an adaptive LPV controller for active microgravity vibration isolation. Both the LPV controller and the antiwindup gain are scheduled based on the measurement of the rack displacement. The design approach followed a classical two-step antiwindup paradigm. Numerical simulations have been used to illustrate the effectiveness of the antiwindup design.

References

[1] Knopse, C. R., Hampton, D. R., and Allaire, P. E., "Control Issues of Microgravity Vibration Isolation," *Acta Astronautica*, Vol. 25, No. 11, 1991, pp. 687–697.

[2] Hampton, D. R., Knopse, C. R., and Grodsinsky, C. M., "Microgravity Isolation System Design: A Modern Control Synthesis Framework," *Journal of Spacecraft and Rockets*, Vol. 33, No. 1, 1996, pp. 110–119.

[3] Grodsinsky, C. M., and Whorton, M. S., "Survey of Active Vibration Isolation Systems for Microgravity Applications," *Journal of Spacecraft and Rockets*, Vol. 37, No. 5, 2000, pp. 586–596.

[4] Fialho, I. J., "H_∞ Control Design for the Active Rack Isolation System," *Proceedings of the American Control Conference*, Institute of Electrical and Electronics Engineers, Piscataway, NJ, 2000, pp. 2082–2086.

[5] Mehendale, C. S., Fialho, I. J., and Grigoriadis, K. M., "A Linear Parameter-Varying Framework for Adaptive Active Microgravity Isolation," *Proceedings of the American Control Conference*, Institute of Electrical and Electronics Engineers, Piscataway, NJ, 2003, pp. 1452–1457.

[6] Aström, K. J., and Wittenmark, B., *Computer Controlled Systems: Theory and Design*, Prentice–Hall, Englewood Cliffs, NJ, 1994.

[7] Campo, P., and Morari, M., "Robust Control of Processes Subject to Saturation Nonlinearities," *Computers and Chemical Engineering*, Vol. 14, No. 4–5, 1990, pp. 343–358.

[8] Bernstein, D., and Michel, A., "A Chronological Bibliography on Saturating Actuators," *International Journal of Robust and Nonlinear Control*, Vol. 5, No. 5, 1995, pp. 375–380.

[9] Hu, T., and Lin, Z. (eds.), *Control Systems with Actuator Saturation: Analysis and Design*, Birkhauser, Boston, MA, 2001.

[10] Kapila, V., and Grigoriadis, K. (eds.), *Actuator Saturation Control*, Marcel Dekker, New York, 2001.

[11] Teel, A., and Kapoor, N., "The L_2 Antiwindup Problem: Its Definition and Solution," *Proceedings of the Fourth European Control Conference*, European Union Control Association, Paris, France, 1997.

[12] Grimm, G., Hatfield, J., Postlehwaite, I., Teel, A., Turner, M., and Zaccarian, L., "Antiwindup for Stable Linear Systems With Input Saturation: An LMI-Based Synthesis," *IEEE Transactions on Automatic Control*, Vol. 48, No. 9, 2003, pp. 1509–1524.

[13] Teel, A., "Antiwindup for Exponentially Unstable Linear System," *International Journal of Robust and Nonlinear Control*, Vol. 9, No. 10, 1999, pp. 701–716.

[14] Wu, F., Grigoriadis, K., and Packard, A., "Antiwindup Controller Design Using Linear Parameter-Varying Control Methods," *International Journal of Control*, Vol. 73, No. 12, 2000, pp. 1104–1114.

[15] Wu, F., and Lu, B., "Antiwindup Control Design for Exponentially Unstable LTI Systems with Actuator Saturation," *Systems and Control Letters*, Vol. 3/4, 2004, pp. 305–322.

[16] Lu, B., Wu, F., and Kim, S., "LPV Antiwindup Compensation for Enhanced Flight Control Performance," *Journal of Guidance, Control, and Dynamics*, Vol. 28, No. 3, 2005, pp. 494–505.

[17] Apkarian, P., and Adams, R., "Advanced Gain-Scheduling Techniques for Uncertain System," *IEEE Transactions on Control Systems Technology*, Vol. 6, No. 1, 1998, pp. 21–32.

[18] Hindi, H., and Boyd, S., "Analysis of Linear Systems with Saturation Using Convex Optimization," *Proceedings of 37th IEEE Conference on Decision and Control*, Institute of Electrical and Electronics Engineers, Piscataway, NJ, 1998, pp. 903–908.

[19] Zhou, K., and Doyle, J., *Essentials of Robust Control*, Prentice–Hall, Upper Saddle River, NJ, 1997.